

Experiments on Bubble Behavior in a Horizontal Narrow Divergent Passage

メタデータ	言語: English 出版者: 公開日: 2008-11-05 キーワード (Ja): キーワード (En): 作成者: OHTA, Junichi, KOKETSU, Mitsuyuki, YAMAMOTO, Fujio メールアドレス: 所属:
URL	http://hdl.handle.net/10098/1762

Manuscript for Heat Transfer Japanese Research

表題 EXPERIMENTS ON BUBBLE BEHAVIOR IN A HORIZONTAL
NARROW DIVERGENT PASSAGE

著者及所属 Junichi Ohta, Mitsuyuki Koketsu, and Fujio Yamamoto
Department of Mechanical Engineering, Faculty of Engineering,
Fukui University
3-9-1, Bunkyo, Fukui-shi 910, JAPAN

Terushige Fujii
Department of Mechanical Engineering, Faculty of Engineering,
Kobe University
1-1, Rokkodai, Nada, Kobe, 657, JPAPAN

原報 Translated from Transaction of JSME (B) **61**,581, pp.201-207(1995)

翻訳者名 by Junichi Ohta
Department of Mechanical Engineering, Faculty of Engineering,
Fukui University

及宛先 3-9-1, Bunkyo, Fukui-shi 910, JAPAN
Tel: +81-776-27-8792
Fax: +81-776-27-8748
E-mail: ohta@fv.mech.fukui-u.ac.jp

ABSTRACT- This paper investigates a bubble which is placed such that it bridges a cross section of a horizontal narrow divergent passage under the Earth gravity condition (1-G). In a narrow passage, inertia forces are known to be small compared with viscous forces. Also, gravity force is not dominant in bubble behavior in a horizontal narrow passage under the 1-G condition. In this sense, the bubble behavior in the passage is similar to that under a low-gravity condition. It is important to understand the bubble behavior in relation to separating gas from a gas-liquid two-phase flow and controlling a gas-liquid interface under a low-gravity condition. A single bubble is placed so under the 1-G condition. The bubble geometry and its behavior are studied experimentally for gap sizes ranging from 0.5 mm to 2 mm, the divergent angles of 1° to 5° , and using ethyl alcohol as a working fluid. The following results are obtained: (1) the bubble is found to move to the greater cross-sectional area; (2) the gas-liquid interface geometry in the top view can be expressed as a “contact circle model” which takes the maximum radius in the passage; and (3) effects of the gap size and the projected bubble area on the bubble behavior are clarified.

Key words: Bubble, Surface tension, Low-gravity, Meniscus, Hele-Shaw Cell, Separation, Narrow Space

1. INTRODUCTION

Recently, a two-phase flow loop has attracted attention as one of advanced thermal management technologies in a space station or a space base ⁽¹⁾. In the thermal management device, the liquid is partially vaporized in a heated section and the vapor is condensed in a cooled section, the heat being transferred as latent heat. In the device, it is necessary to control the gas-liquid interface and to separate the gas from the two-phase flow under a microgravity condition. Separation of bubbles was carried out under a microgravity condition using a wire mesh by Fujiwara et al. ⁽²⁾ and using surface tension by Furukawa et al. ⁽³⁾. Also,

transportation of a bubble was conducted using ultrasonic waves by Anoda et al ⁽⁴⁾ and using static electricity by Imai et al. ⁽⁵⁾.

When a bubble is placed to bridge a cross section of a divergent passage, surface tension may causes the bubble to move to greater cross-sectional area ⁽⁶⁾⁽⁷⁾. If the distribution of the cross-sectional area is varied along the passage direction during operation, this variation may allow the bubble in the passage to move to the direction of the greater cross-sectional area and to control the bubble location under a microgravity condition. In a horizontal narrow channel, inertia force is known to be small compared with viscous force ⁽⁸⁾. Gravity force is not dominant for bubble behavior in the horizontal narrow channel under the 1-G condition. In this sense, the bubble behavior in the channel is considered to be similar to that under a microgravity condition. There were studies ⁽⁹⁾⁽¹⁰⁾ about behavior of a bubble in a narrow channel. In these studies, bubbles are located apart from the side walls. In the present study, however, a bubble is placed to bridge the cross section of the horizontal narrow channel.

The purpose of this study is to clarify the shape and the behavior of the bubble which bridges the cross section of the horizontal narrow divergent passage under the Earth gravity condition (1-G) experimentally. The present study focuses on the observation and the measurement, and a theoretical analysis of the bubble behavior will be described in a subsequent paper.

NOMENCLATURE

h	: Gap size in a side view
k	: The ratio of an area where a bubble touches a side wall to an area of the bubble in the side view
R	: A radius of curvature for a gas-liquid interface in a top view (see Fig.4)
S	: Bubble area projected on a top view

- X : Axial length from the converging point (see Fig. 4)
- X_u : Upstream interfacial location (see Fig. 4)
- ϕ : Divergent angle (angle between the center line and the spacer for passage;
see Fig.4)
- σ : Surface tension

SUBSCRIPT

- u : Upstream side (side of smaller cross-sectional area)
- d : Downstream side (side of greater cross-sectional area)

2. EXPERIMENTAL APPARATUS AND PROCEDURE

Three kinds of experimental apparatus, i.e. apparatus A, apparatus B, and apparatus C, were made in the present study. First, a top view and a side view of apparatus A are shown for measuring bubble shape and its behavior in Fig. 1. It consists of two transparent thick plates (width x length x thickness: 100 mm x 250 mm x 15 mm), two thin plates (length x width x thickness: 110 mm x 10 mm x h mm; these are called spacers for passage), and five thin plates surrounding the inner liquid (thickness, i.e. gap size h) for the circumference. All of the experimental apparatus were made of acrylic resin. Note that a narrow divergent passage of interest in the present study is surrounded with the two thick plates and the two thin spacers for passage. To inject a bubble into the passage, a rectangular hole was made and surrounded with the two left side circumference spacers and the two thick plates. Nine apparatus, i.e. four apparatus for the bubble behavior and five apparatus for the bubble shape measurement, were made as apparatus A and their specifications are given in Table 1.

Secondly, a top view of apparatus B is shown in Fig. 2. Apparatus B was made for

clarifying an effect of the two side passages on the bubble movement. The side passages are blocked in apparatus B by four spacers (thin plates) as shown in Fig. 2. Apparatus B is the same shape as apparatus A for the divergent angle ϕ of 2.8° and h of 1.0 mm except the side passages. Thirdly, apparatus C was made to visualize the bubble shape from the side as shown in Fig. 3. Apparatus C has a divergent angle ϕ of 3.25° and also its dimensions are shown in Fig. 3.

Definitions of variables are shown in Fig. 4. From the figure, upstream interface location X_u denotes the shortest gas-liquid interface location from the extended converging point in this paper. The side of smaller cross-sectional area and the side of greater cross-sectional area are called upstream and downstream, respectively, for convenience.

One of the experimental apparatus was placed horizontally on a bed whose inclination could be adjusted precisely. Experiments were carried out using commercial use ethyl alcohol (concentration of 99.5 %) as a working fluid under temperatures of 287 to 293 K in a room where the temperature could be controlled. Before experiments, the experimental apparatus was washed using the ethyl alcohol which was the same liquid as the working fluid. An experimental procedure is as follows: (1) The bed was adjusted to make the experimental apparatus horizontal. (2) The experimental apparatus was filled with the ethyl alcohol. (3) Air was injected into the divergent passage through the rectangular hole slowly with an injector to produce a bubble. (4) The injector was pulled out and the hole was closed. (5) After it took several minutes for the bubble to come to rest in the passage by inclining the experimental apparatus, it was replaced. (6) When the apparatus started to be replaced from the inclined position (the bubble was at rest at inclination angles ranging from 0.5° to 1.0°) to horizontal, the time was taken as 0 s^{**1} . The behavior of the bubble was recorded with a video camera or a camera in reflected or transmitted illumination.

3. EXPERIMENTAL RESULTS AND DISCUSSIONS

3.1 General Behavior of a Gas Bubble and Its Shape

3.1.1 General Behavior of a Gas Bubble

When a bubble was moving in the divergent narrow passage for apparatus A ($\phi = 2.8^\circ$ and $h = 2.0$ mm), pictures were taken in reflected illumination. The behavior of the bubble is shown with time on the right hand side of the pictures in Fig. 5 (a). In these pictures, the bubble interface and the two divergent passage spacers look white, while the ethyl alcohol and the inside of the bubble look black. From the pictures, the bubble moves to the greater cross-sectional area, a part of the bubble comes out of the passage, and the part expands in the outside of the passage, as time passes. Furthermore, the bubble departs from the passage, moves downstream due to the inertia, and comes to rest, as time passes. The upstream interfacial location was read from the photographs corresponding to Fig. 5 (a) every 30 seconds. The upstream interfacial location X_u was plotted against time in Fig. 5 (b). From the figure, the interfacial velocity decreases as the bubble goes downstream.

In the case that there was another big bubble outside the passage, pictures of the bubble behavior in the divergent passage were taken in transmitted illumination as shown in Fig. 6. In the pictures, the bubble interface and the divergent passage spacer look black, while the ethyl alcohol looks gray. The ellipse and the region inside of the right arc represent the inside bubble of the passage and the outside bubble, respectively. As time passes, the inside bubble comes out of the passage and then the inside bubble and the outside bubble coalesce. This means that the gas can be separated. Since there is a possibility that the outside bubble affects the inside bubble behavior, experimental data without the outside bubble is presented from the next section.

3.1.2 Bubble Shape

It is necessary to clarify the gas-liquid interfacial shape and the structure between the bubble and the side wall (the spacer for passage) through observation and measurement in

**1 It took about 0.7 s for the apparatus to remove from inclined position to horizontal position.

order to understand the bubble behavior and its mechanism. The observations and the discussions will be described below.

(1) The gas-liquid interface shape from the top

A magnified bubble picture from the top is shown in Fig. 7. Since the shape of upstream and downstream interfaces can be assumed to be maximum circles, respectively, which can be put into the divergent channel, this model is proposed and called "contact circle model" in this paper. Applying the model to a bubble, a relationship between the upstream interface, X_u , and the upstream radius of curvature, R_u , is given by Eq. (1) (see Fig. 4).

$$R_u = X_u \frac{\sin \phi}{1 - \sin \phi} \quad (1)$$

Also, a relationship between the downstream interface, X_d , and the downstream radius of curvature, R_d , is expressed as Eq. (2).

$$R_d = X_d \frac{\sin \phi}{1 - \sin \phi} \quad (2)$$

To verify the "contact circle model", the relationship between R_u and X_u and the relationship X_d and R_d were obtained by measuring eleven coordinates on the interface for each magnified picture with a microscope. Measured R_u and R_d are plotted against X_u and X_d , respectively, with divergent angles as the parameter in Fig. 8 (a) and with gap size as the parameter in Fig. 8 (b). Also, calculated results for Eqs. (1) and (2) are shown by solid and dashed lines, respectively, in the figures. From Figs. 8 (a) and (b), it is seen that measured values are in good agreement with calculated those and are independent of the gap size. The reason may be that deviations from a circular are considerably small due to the low gas-liquid interfacial velocity. Therefore, it is concluded that the contact circle model is appropriate to these cases.

(2) Gas-liquid interface shape in the side view

Boundary regions between a bubble and the side wall of the spacer for passage were observed from the top of apparatus A in transmitted illumination with the microscope which has a minimum scale of 1 μ m. However, a liquid film could not be observed between the bubble and the side wall as long as we used the microscope. When a bubble was placed in the divergent passage for apparatus C, a side view of the bubble picture was taken in transmitted illumination. The photograph is indicated in Fig. 9. A variable of k denotes the ratio of a bubble area touching the side wall to the bubble area projected on the side view, i.e. $h (X_2 - X_1) / \cos \phi$.

A gas-liquid interface shape from the side was measured with experimental apparatus C for $h = 1$ mm (Fig. 3) using the same procedure as the measurement for the interface from the top. The results approximated to circles are shown in Fig. 10. As seen from the figure, the upstream curvatures of radius are greater than downstream ones by 0 to 0.1 mm.^{**2}

^{**2} Figure 10 shows that the upstream radius of curvature tends to greater than the downstream radius of curvature. When the pressure difference between the upstream liquid and the downstream liquid can be negligible, this is explained as follows:

With use of symbols in Fig. 4, the Laplace equation gives

$$\begin{aligned} P_i - P_d &= \sigma \left(\frac{1}{R_d} + \frac{1}{R_{d,s}} \right) \\ P_i - P_u &= \sigma \left(\frac{1}{R_u} + \frac{1}{R_{u,s}} \right) \\ P_d - P_u &= \sigma \left(\frac{1}{R_u} - \frac{1}{R_d} + \frac{1}{R_{u,s}} - \frac{1}{R_{d,s}} \right) \end{aligned}$$

$P_d - P_u = 0$ is assumed

$$\frac{1}{R_u} - \frac{1}{R_d} = \frac{1}{R_{d,s}} - \frac{1}{R_{u,s}}$$

where P_i , P_u , and P_d are pressures in the bubble, in the upstream liquid, and in the downstream liquid. R_u , R_d , $R_{u,s}$, and $R_{d,s}$ are radii of curvature for upstream from the top, downstream from the top, upstream from the side, and downstream from the side, respectively. Since $R_u < R_d$ is obvious,

Hence

$$\frac{1}{R_u} > \frac{1}{R_d}$$

$$\frac{1}{R_{d,s}} - \frac{1}{R_{u,s}} > 0$$

$$R_{u,s} > R_{d,s}$$

3.2 Effect of Various Factors

3.2.1 Effect of the Gap Size from the Side

To discuss the influence of the gap size on the bubble behavior, measured upstream interfacial locations of bubble X_u are shown with time for the gap sizes h of 0.5, 1.0 and 2.0 mm, projected bubble areas S of 129, 142, and 128 mm², divergent angle ϕ of 2.8°, and temperatures of 288.7 to 290.2 K in Fig. 11. From the figure, it is found that the upstream interfacial location moves faster as the gap size becomes greater. This is explained as follows. An effective driving force, Eq. (5), exerts on the bubble by the side wall of the spacer for passage, as will be mentioned in subsection 3.2.5. The pressure difference in Eq. (5) can be given by the Laplace's equation.

$$\Delta P \doteq \sigma \left(\frac{2}{h} + \frac{1}{R} \right)$$

Substituting the Laplace's equation into Eq. (5), the effective driving force becomes

$$F_d \doteq 2 \cdot k \cdot \sigma \left(2 + \frac{h}{R} \right) \cdot (X_2 - X_1) \tan \phi \quad (3)$$

For a laminar flow, a wall friction force in two-dimensional parallel plates can be expressed as

$$F_\tau = \frac{12\nu\bar{u}S_e}{h} \quad (4)$$

where u , S_e , and ν are the average liquid velocity, area of the ethyl alcohol touching the parallel plates, and kinematic viscosity, respectively. When Eqs. (3) and (4) are compared for the same bubble location, the constant projected bubble area S , and negligibly small change in k , the driving force Eq. (3) becomes greater and the wall friction force Eq. (4) decreases as the gap size increases. This may be considered to be a primary reason that the bubble moves

It has been explained that the upstream radius of curvature is greater than the downstream radius of curvature.

faster as the gap size increases.

3.2.2 Effect of the Projected Bubble Area on the Top View

To examine the influence of the projected bubble area on the bubble behavior, the upstream interfacial locations X_u are shown with time for the gap size h of 1 mm, divergent angle ϕ of 2.8° , and projected bubble areas S of 76, 142, 238, and 322 mm² in Fig. 12. From the figure, it is seen that the upstream interfacial location moves faster, as the projected bubble area becomes greater. The cause may be explained as follows. This is considered to relate to Eq. (5), i.e. the effective force by the side wall acting on the bubble. As the projected bubble area becomes greater, the bubble area touching the side wall, i.e. $(k h (X_2 - X_1) / \cos \phi)$, increases. Thus, the force in Eq. (5) increases with projected bubble area.

3.2.3 Effect of the Divergent Angle

The upstream interfacial locations are shown with time at h of 1 mm for ϕ of 1.0° and S of 80 mm² and for ϕ of 2.8° and S of 76 mm² in Fig. 13. It is seen that the upstream interface in the case of ϕ of 1.0° moves faster than that for ϕ of 2.8° at S of around 80 mm². Since the bubble does not move for ϕ of 0° , it is expected that there is a divergent angle which gives the maximum interfacial velocity for a constant projected surface area. Also, the force of Eq. (5) takes the maximum against the divergent angle for a constant projected surface area. For $S \doteq 80$ mm², an amount of the ethyl alcohol occupied in the divergent passage at ϕ of 2.7° is greater than that at ϕ of 1° . This means that the greater amount of the ethyl alcohol in the divergent passage must be transported for ϕ of 2.8° . Thus, the bubble movement for various divergent angles is considered to be affected by many experimental factors.

3.2.4 Effect of the Side Passages

Liquid downstream of the bubble must be transported to the upstream section during

the bubble movement in apparatus A, since the apparatus is type of closed space. The two cases are expected as follows. (a) There are four corner gaps between the bubble and the inner wall in the cross section of the divergent passage. The liquid in the downstream section may be transported through the four corner gaps to the upstream section. (b) Liquid in the downstream section may move through the side passage of the experimental apparatus to the upstream section. Thus, similar experiments were carried out using apparatus B in which the side passages are blocked. The upstream locations X_u are shown in Fig. 14 with the side passages by solid symbols, which are the same as those in Figs. 11 to 13, and without the side passages by open symbols. From Fig. 14, it is seen that the upstream interfacial location with the side passages moves much faster than that without the side passages. Also, it should be noted that the bubble moves even if the side passages are blocked. It is concluded that the liquid in the downstream section is transported to the upstream through the two ways of (a) and (b), as mentioned above, however the flows in the side passages are dominant in the bubble movement.

3.2.5 Force Caused by Pressure Difference between the Bubble and the Liquid

A pressure difference at the gas-liquid interface of the bubble may be given by Laplace's equation due to the low interfacial velocity. Hence, the pressure in the bubble, P_i , is higher than that for the surrounding liquid. Part of the bubble is assumed to touch the side wall of the spacers for passage, as mentioned above in subsection 3.1.2. Thus, the pressure in the bubble, P_i , is equal to that on the side wall P_s where the bubble appears to touch. In other words, the bubble is pushed in the area touching the side wall, in the normal direction of the side wall, by the side wall at P_i . Therefore, the side wall pushes the bubble, the bubble pushes the surrounding liquid, and the bubble behaves like a piston pushing the liquid due to the bubble pressure higher than the liquid pressure. Because of the low liquid velocity, the liquid pressure in the vessel can be considered to be constant, i.e. the liquid pressure difference between upstream and downstream of the bubble can be negligible, the effective

force component in the axial direction acting on the bubble can be expressed as

$$F_d = 2 \cdot \Delta P \cdot k \cdot h(X_2 - X_1) \tan \phi \quad (5)$$

where ΔP : the pressure difference between the gas and the liquid; $k h (X_2 - X_1) / \cos \phi$: the area where the bubble touches the side wall as mentioned in subsection 3.1.2 (2).

As seen from Eq. (5), this force directs to the larger cross-sectional area of the divergent passage. Therefore, the bubble moves to the larger cross-sectional area. Also, Eq. (5) can explain the effects of gap size, projected bubble area, and divergent angle on the bubble movement qualitatively as mentioned above in subsections 3.2.1 to 3.2.4. However, further studies are expected, since there is a possibility that other forces act on the bubble.

4. CONCLUSIONS

Behavior and shape of a single bubble which was placed to bridge a cross section of a horizontal narrow divergent passage were observed and measured under the Earth gravity condition using ethyl alcohol as a working fluid, from the point of view of a basic study for technologies of separating gas and maintaining liquid under a low-gravity condition. The results are summarized as follows:

- (1) The bubble moves to the greater cross-sectional area.
- (2) The gas-liquid interface shape in the top view is confirmed to be expressed as a “contact circle model” which takes the maximum radius in the passage.
- (3) Effects of the gap size and the projected bubble area are clarified on the bubble behavior.
- (4) Flows in the side passages are dominant in the bubble behavior.

Acknowledgement

The authors would like to express their thanks to Messrs. Yuji AKASHI, Ryuji OKADO, and Masa-aki ODA, students at Fukui University, for their cooperation in the experiments.

REFERENCES

- (1) Fujii, T. and Ohta, J., *Lecture series for Japan Society of Multiphase Flow*, No.5, (1990) pp.63-85. (in Japanese).
- (2) Fujiwara, M., Toyofuku, M., Watanabe, M., Watanabe, S., and Suzuki, K., *Proc. of 27th National Heat Transfer Symposium of Japan*, (1990) pp. 685-687. (in Japanese)
- (3) Furukawa, M., Ishii, Y., Miyazaki, Y., Iida, T., Report on Power Station System and Thermal Management System in Space (P-SC194) by JSME, (1993) pp. 111-119.(in Japanese)
- (4) Anoda, Y., Watanabe, T., and Kukita, Y., *Proc. The International Conference on Multiphase Flows '91-Tsukuba*, (1991) pp.397-400.
- (5) Imai, R., and Yano, T., *Proc. of Japan Society of Mechanical Engineer (II)*, No. 930-9, (1993) pp.388-390. (in Japanese)
- (6) Ohta, J., Fujii, T., Ueda, S., Yamamoto, F., *Proc. 2nd JSME-KSME Thermal Engineering Conference*. (1992), pp.265-270.
- (7) Ohta, J., Fujii, T., and Yamamoto, F., *Proc. Multiphase Flow Symposium '93*, (1993) pp.185-188. (in Japanese)
- (8) Batchelor, G.K., *An Introduction to Fluid Dynamics*, Cambridge University Press, (1967).
- (9) Taylor, G., and Saffman P.G., *Quart. J. Mech. And Applied Math*, Vol. XII, Pt. 3, (1959) pp. 265-279.
- (10) Moriyama, K., Inoue, A., *Trans. Japan Society of Mechanical Engineers (B)*, **59**, 560 (1993) pp.1003-1011. (in Japanese)

FIGURES AND TABLE LIST

Table 1 Specifications of experimental apparatus A

Fig. 1 Experimental apparatus A (with side passages)

Fig. 2 Experimental apparatus B (without side passages)

Fig. 3 Experimental apparatus C (for visualizing a bubble in the side view)

Fig. 4 Definition of symbols

Fig. 5 (a) Picture for bubble behavior

Fig. 5 (b) Relationship between upstream interfacial location and time

(Corresponding to Fig. 5(a))

Fig. 6 Picture for a bubble behavior with another bubble outside the passage

Fig. 7 Enlarged photograph of a bubble in the top view

Fig. 8 (a) Relationship between curvature of radius for interfaces and the interface locations

(Effect of the divergent angle)

Fig. 8 (b) Relationship between curvature of radius for interfaces and the interface locations

(Effect of the gap size)

Fig. 9 Photograph of a bubble in the side view

Fig. 10 Radius of curvature of gas-liquid interface in the side view

Fig. 11 Effect of the gap size on bubble behavior

Fig. 12 Effect of the projected bubble area on bubble behavior

Fig. 13 Effect of the divergent angle on bubble behavior

Fig. 14 Effect of the side passages on bubble behavior

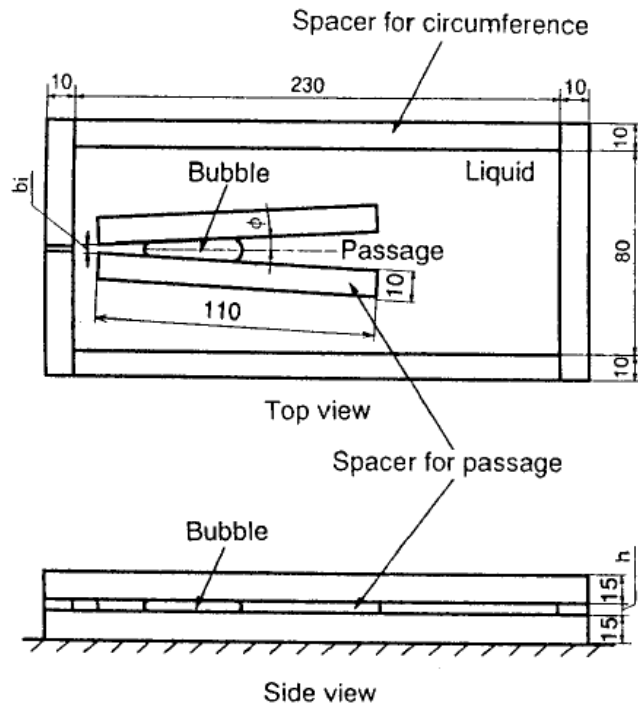


Fig. 1. Experimental apparatus type A (with side passages).

Table 1. Specifications of Experimental Apparatus Type A

	For bubble behavior				For bubble shape measurement				
ϕ (deg)	2.8	2.8	2.8	1.0	1.33	3.13	5.00	3.17	2.73
h (mm)	0.5	1.0	2.0	1.0	1.0	1.0	1.0	0.5	2.0
b (mm)	0.8	0.9	0.7	1.0	1.14	0.78	1.50	1.04	0.73

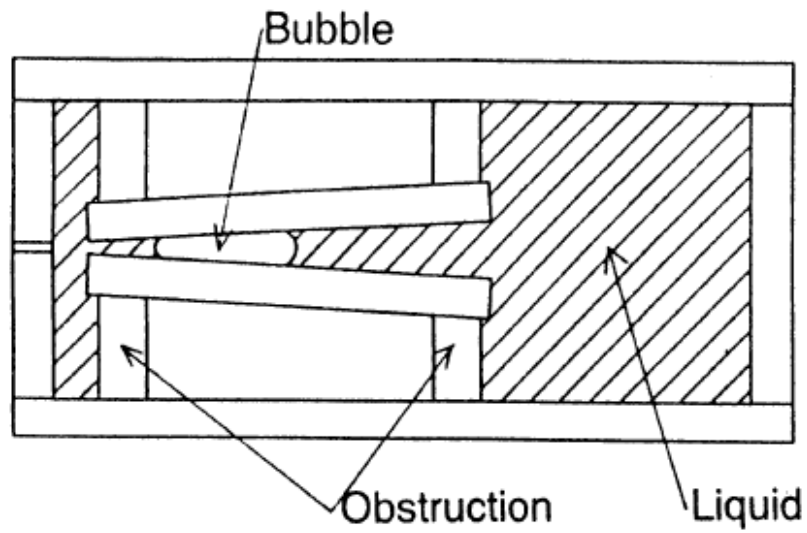


Fig. 2. Experimental apparatus type B (without side passages).

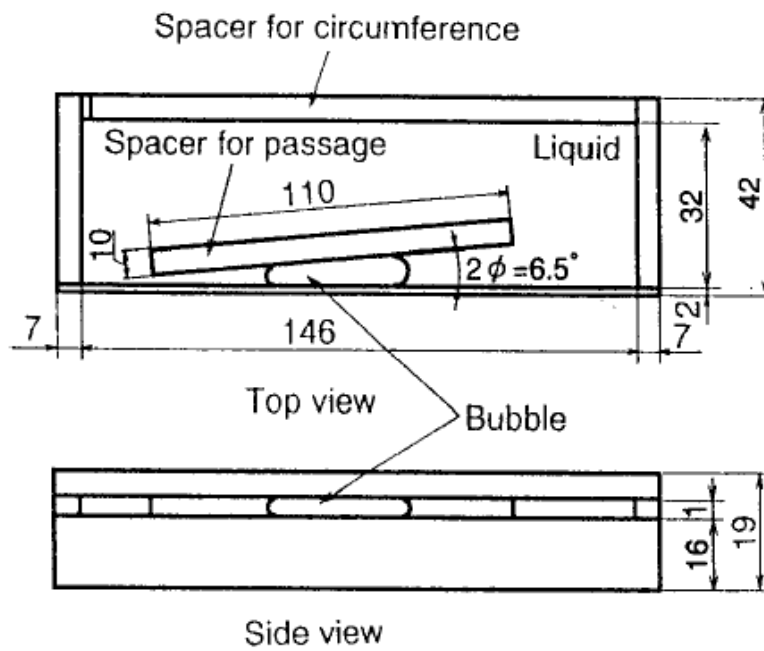


Fig. 3. Experimental apparatus type C (to visualize a bubble in side view).

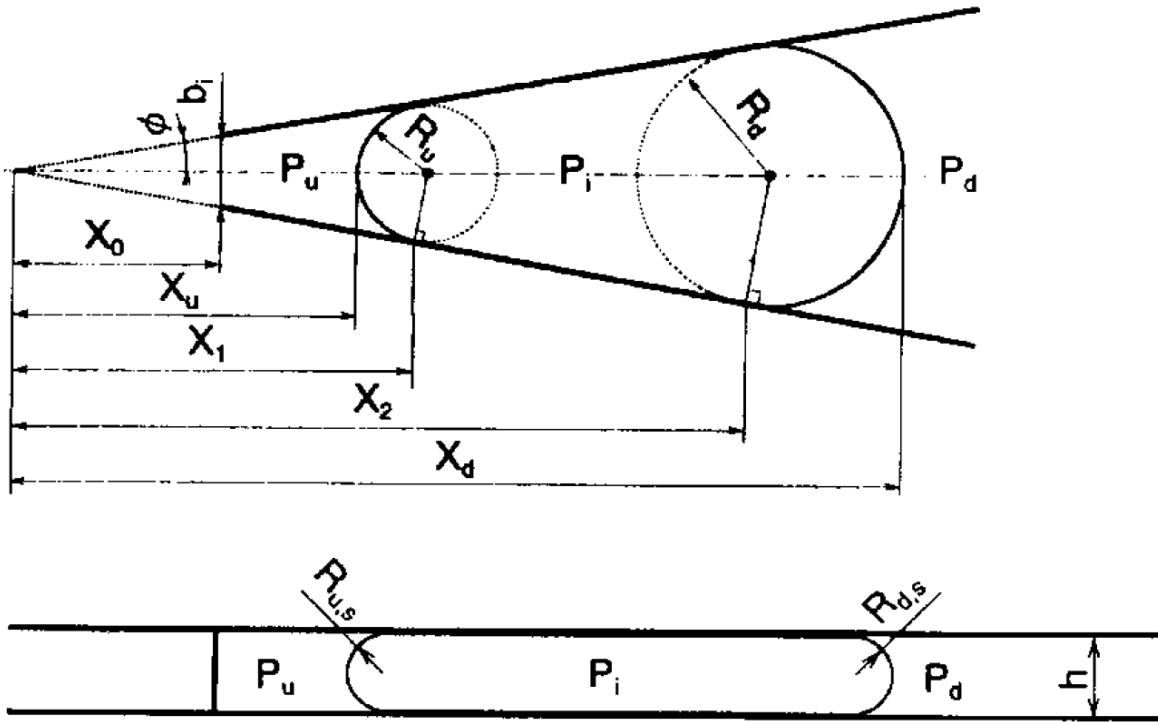


Fig. 4. Definition of symbols.

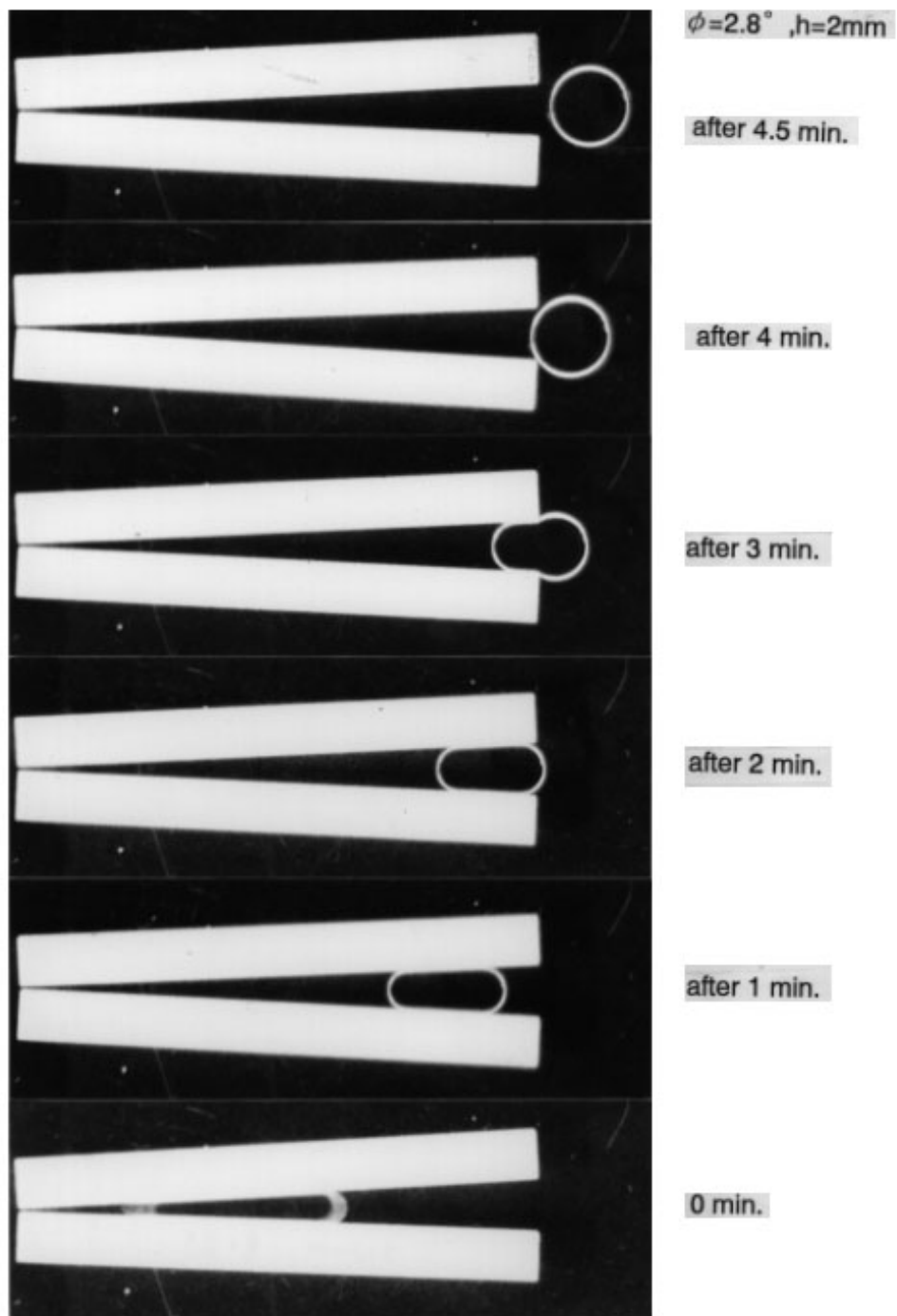


図 5 (a) 流路内気泡の連続写真

Fig.5(a)

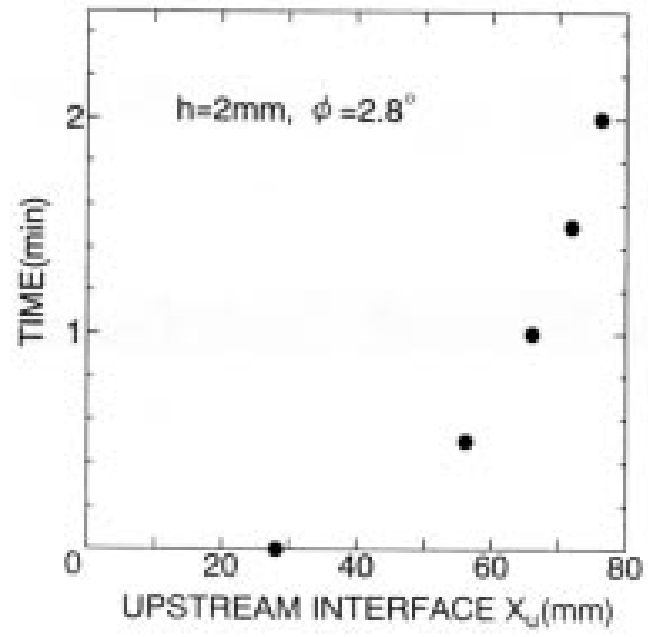


Fig.5(b)

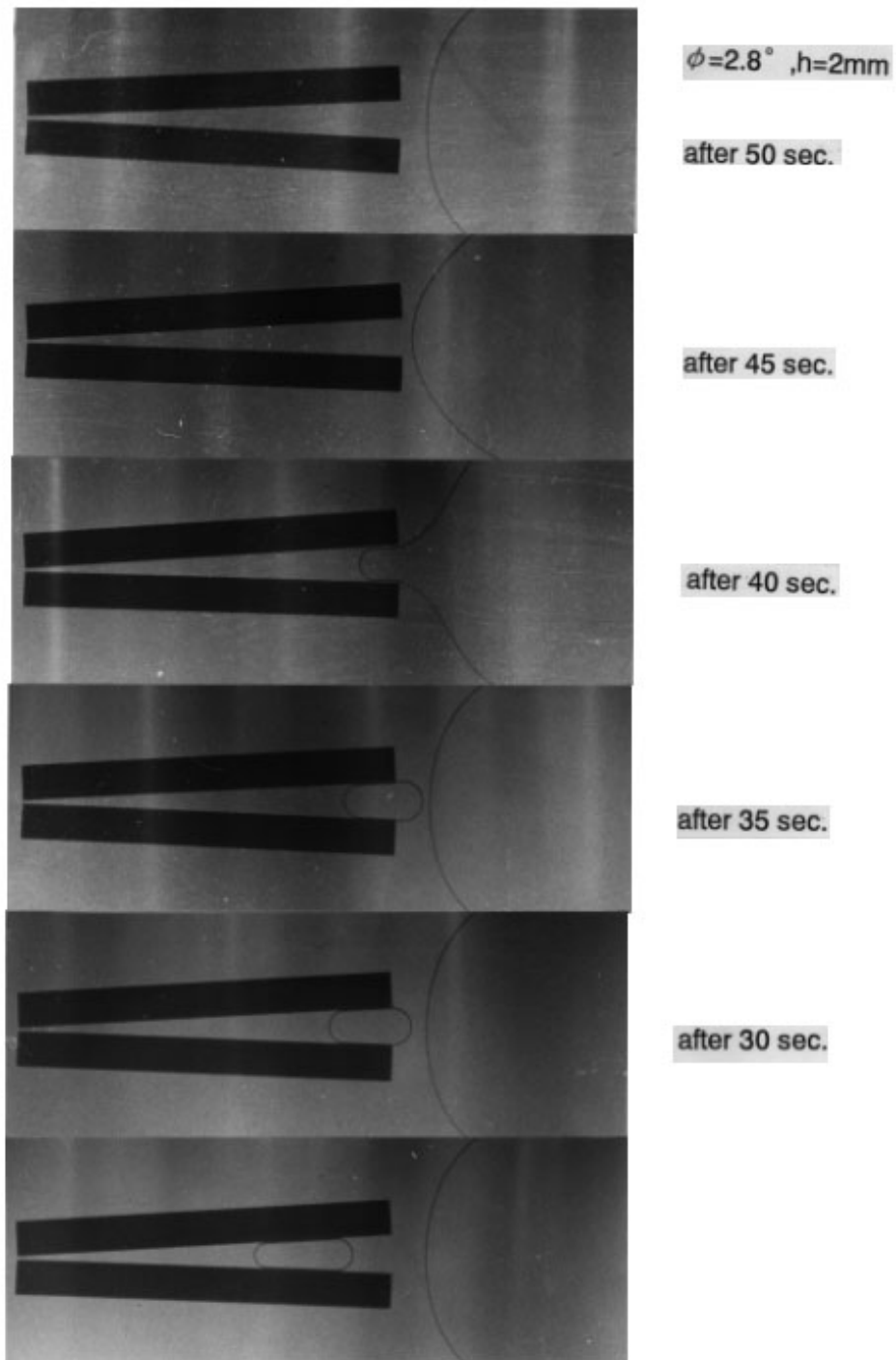


図 6 流路外に気泡のある場合の連続写真

Fig.6

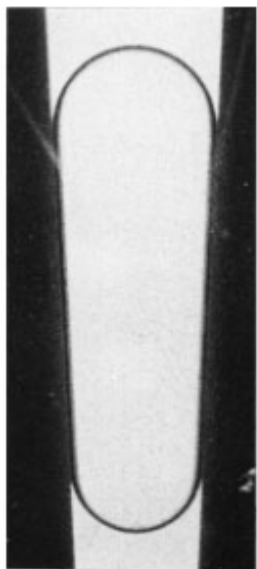


図7 上面から見た気泡の拡大写真

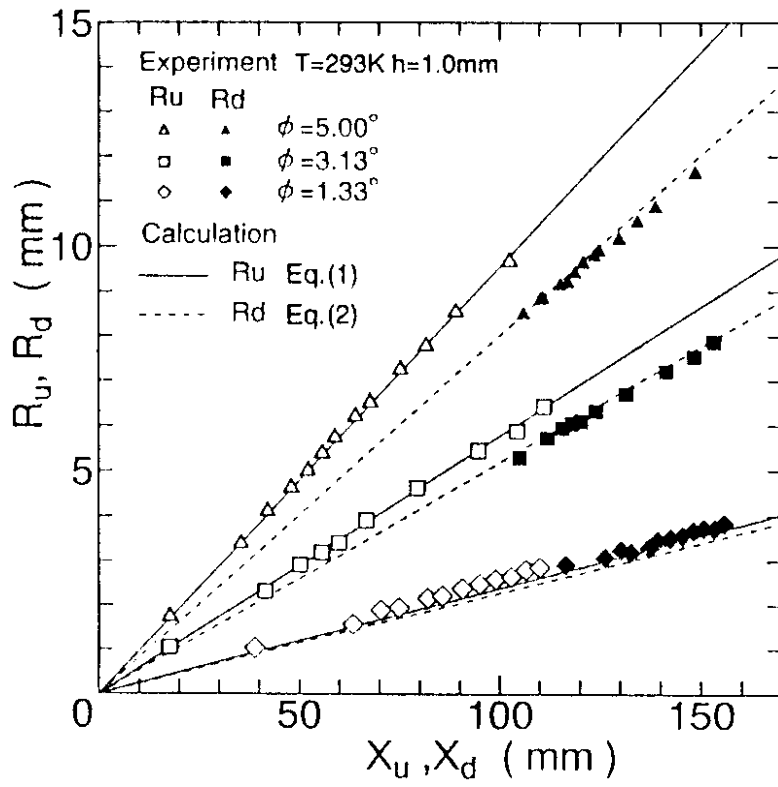


Fig.8(a)

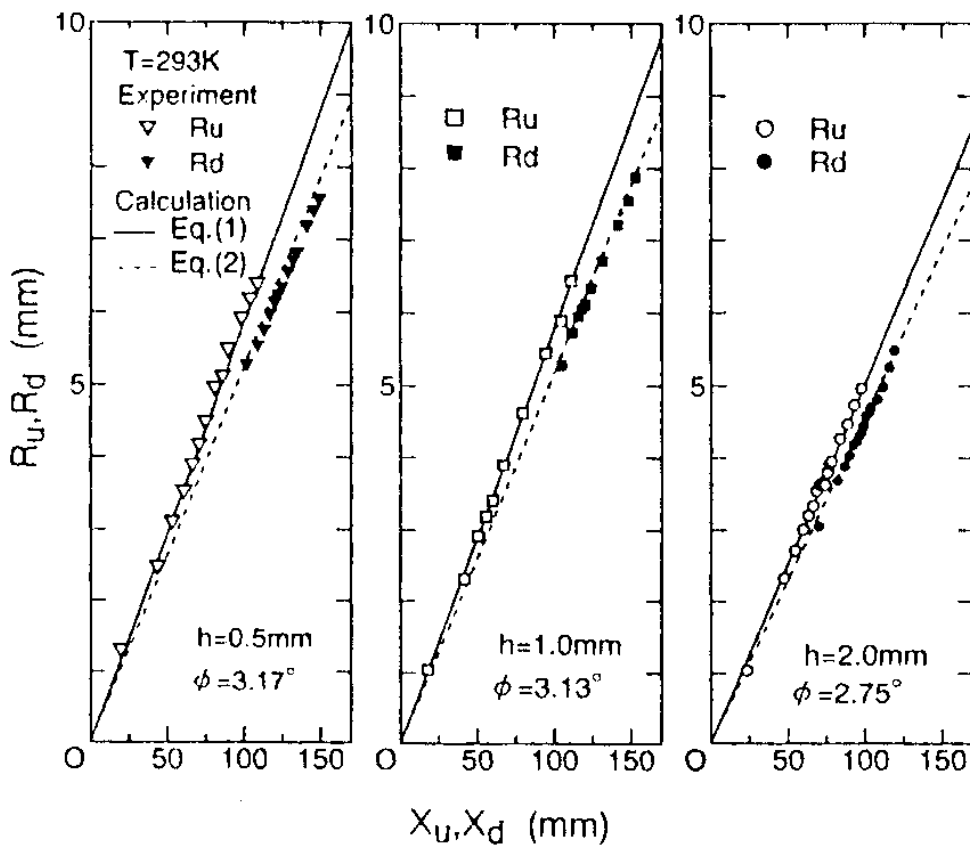


Fig.8(b)

図 9 側面から見た気泡の写真

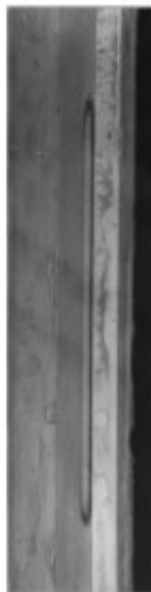


Fig.9

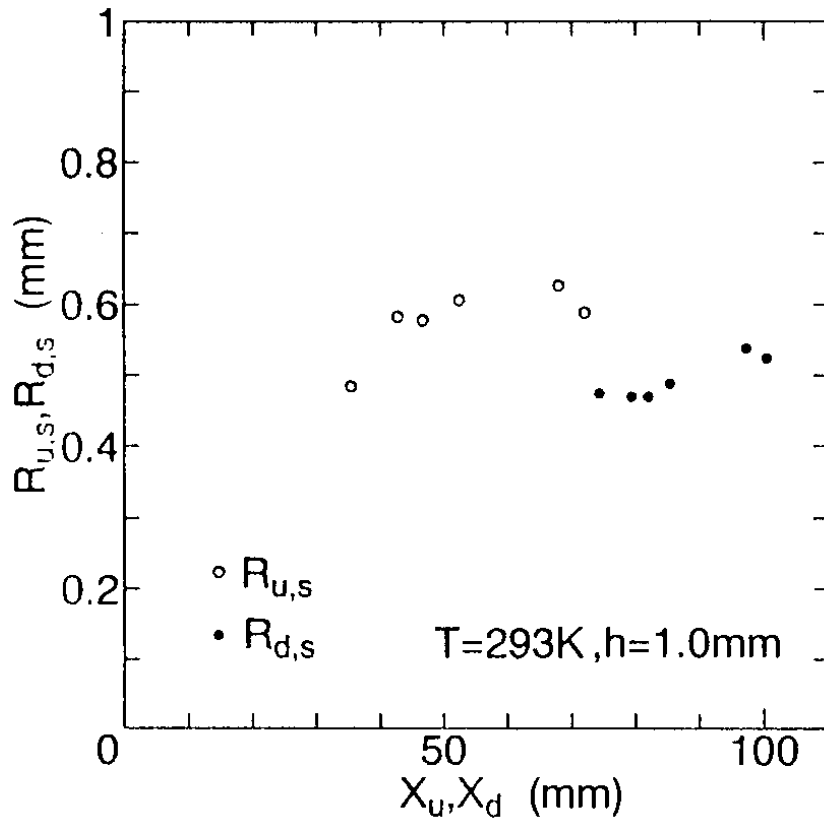


Fig.10

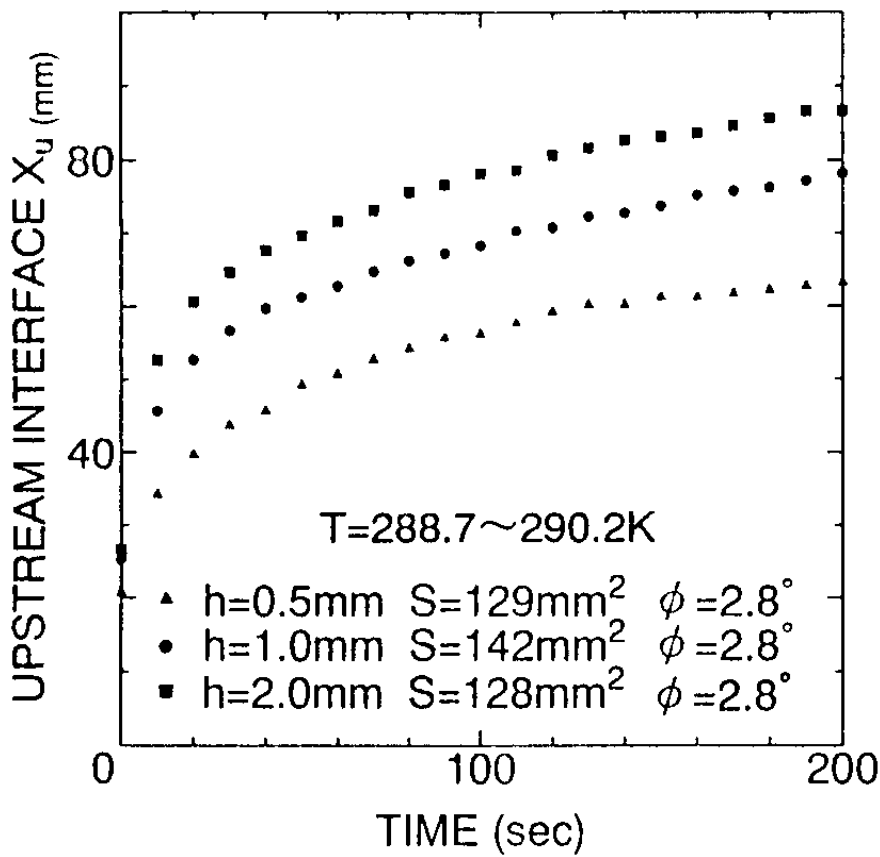


Fig.11

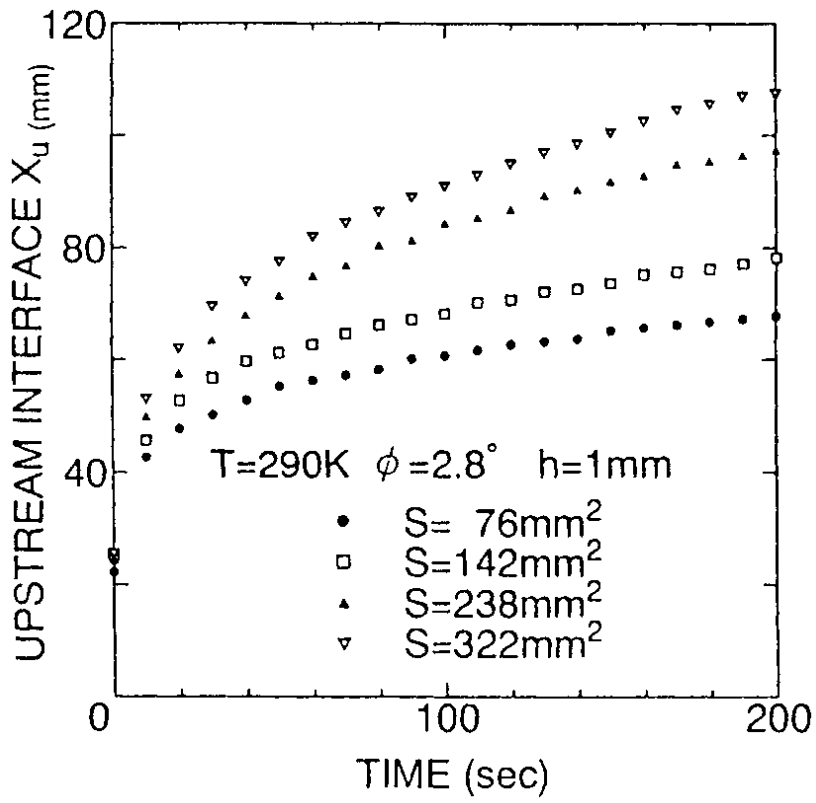


Fig.12

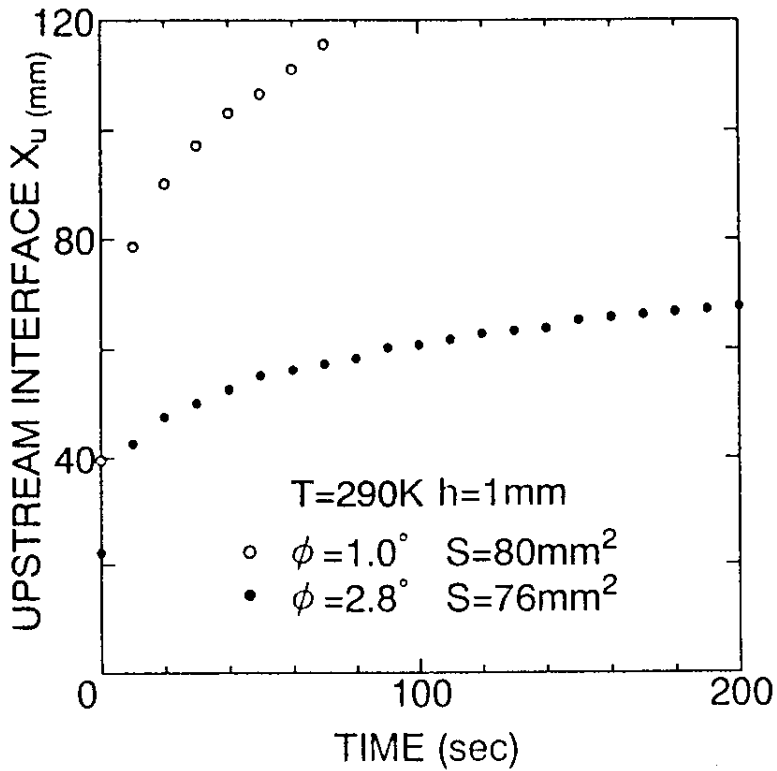


Fig.13

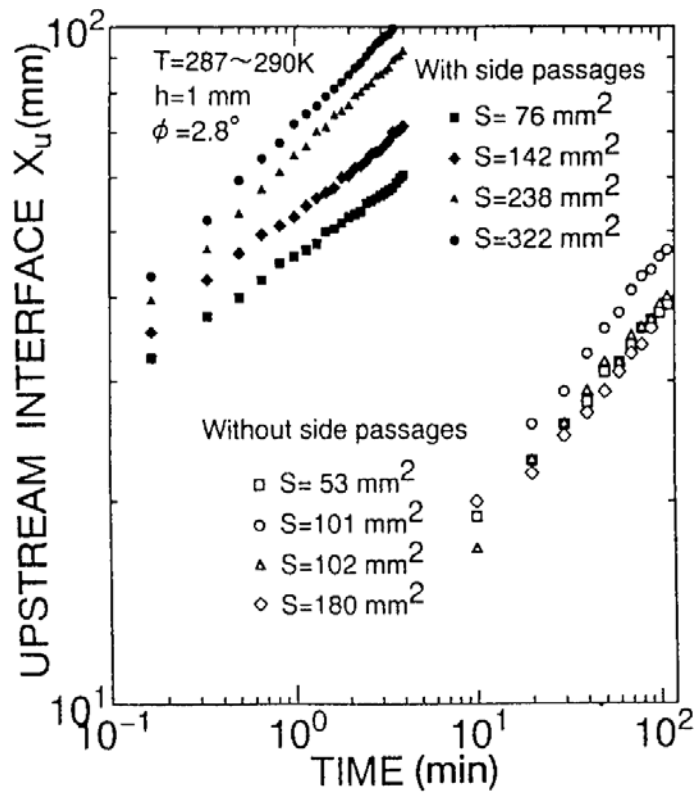


Fig.14